

Quasi symplectic integrators for stochastic differential equations

R. Mannella

Dipartimento di Fisica and INFN, UdR Pisa, Università degli Studi di Pisa, Via Buonarroti 2, 56100 Pisa, Italy

(Dated: December 4, 2003)

Two specialized algorithms for the numerical integration of the equations of motion of a Brownian walker obeying detailed balance are introduced. The algorithms become symplectic in the appropriate limits, and reproduce the equilibrium distributions to some higher order in the integration time step. Comparisons with other existing integration schemes are carried out both for static and dynamical quantities.

PACS numbers: 05.40.-a, 05.10.-a, 05.20.-y, 02.50.-r

I. INTRODUCTION

Stochastic processes are well known to be at the heart of many physical systems [1]. Several approaches have hence been developed to understand the dynamics which is realized given specific models: among others, one of the most used ones is Monte-Carlo integration of the equations of motion.

The literature on the numerical integration of stochastic differential equations is huge: we will limit here to mention a couple of classical citations widely used in the physics community [2–4]. Additional comments and references can be found in [5]. The numerical algorithms presented in these works are general and can be applied to basically any flow; however, they might not be the optimal ones for cases when additional information about the details of the system under study are available.

An important class for which dedicated algorithms can be derived is given by the equations of motion

$$\begin{aligned}\dot{x} &= v \\ \dot{v} &= -\gamma v + F(x) + \xi(t)\end{aligned}\quad (1)$$

where $\xi(t)$ is a random Gaussian noise, with zero average and standard deviation

$$\langle \xi(t)\xi(s) \rangle = 2\gamma T\delta(t-s).$$

In the following, we will also use $V(x)$, defined as $F(x) \equiv -V'(x)$. Note that although we are dealing here with only one Brownian walker, the algorithm we are going to show can be easily extended to the case when x and v are vectors, and $F_i(x)$, the force acting on the i -th walker, is a function of all other walkers.

The above equation is commonly found in the liquid state literature (for numerical schemes appropriate in the integration of the Brownian dynamics of a liquid, see among others [6–10]) and some algorithms have been proposed, over the years, for its numerical integration.

To date, perhaps the most widely used algorithms for the integration of Eq. 1 are the ones derived in [6], where two algorithms have been proposed (see also references therein): we will benchmark against one of them, and to this end, we will briefly review them below. Note that the system of Eq. 1 becomes symplectic when $\gamma \rightarrow 0$ and,

until some recent works [11–13], this symplectic nature was not really exploited in deriving numerical schemes.

The approach we will follow is to derive numerical algorithms having in mind two requirements: (i) the algorithm should become symplectic in the deterministic ($T = 0$) and frictionless ($\gamma = 0$) limit; and (ii) the numerical algorithm should reproduce as closely as possible the equilibrium distribution, when it is defined, of the system given by Eq. 1. As we will see below, to the best of our knowledge either the former or the latter requirements have been enforced in the derivation of numerical schemes, but never both of them. The algorithms introduced here will improve both the algorithms of [6] and of [13].

II. BRIEF REVIEW OF THE BENCHMARK ALGORITHMS AND SOME DEFINITIONS

To assess how well each algorithm is performing, we start from the knowledge that for $V(x)$ which are bounded from below, Eq. 1 leads to an equilibrium distribution $P(x, v)$ for the variables x and v of the form

$$P(x, v) = N \exp \left\{ - \left(v^2/2 + V(x) \right) / T \right\}. \quad (2)$$

where N is a normalization constant. We are going to compare the exact theoretical equilibrium distribution to the equilibrium distribution obtained from the simulations. It is possible, in principle, to check theoretically which is the equilibrium distribution which is expected integrating using a given numerical scheme, following [17]: suppose we have a numerical scheme of the form

$$x_i(t+h) = x_i(t) + hW_i(x_i, \xi)$$

then the probability distribution of x_i satisfies

$$P(x_i, t+h) - P(x_i, t) = \sum_{n=1}^{\infty} \sum_{x_i} \frac{\partial}{\partial x_i} \dots \frac{\partial}{\partial x_n} K_{1\dots n} P(x_i, t) \quad (3)$$

with

$$K_{1\dots n} \equiv (-1)^n \frac{1}{n!} \langle W_1 \dots W_n \rangle_{\xi},$$

where $\langle \dots \rangle_\xi$ means averaging over the noise realizations. In general, for systems in detailed balance at temperature T ,

$$P(x_i, t = \infty)_{sim} = P(x_i, \infty)_{true} \times \exp \left(\sum_{n=1}^{\infty} h^n S_n / T \right)$$

where P_{sim} is the equilibrium distribution generated in the simulations, and P_{true} is the theoretical equilibrium distribution. Given the explicit form of the numerical scheme, the various $K_{1\dots n}$ can be computed: applying Eq. 3, and expanding the r.h.s. of Eq. 3 in the small parameter h , assuming (equilibrium) that $P(x_i, t+h) - P(x_i, t) = 0$, we can derive the equations satisfied by the S_i . The first nonzero S_i yields the correction to the true equilibrium distribution generated by the numerical scheme.

Let us show how to use Eq. 3 taking one of the algorithms of [6]. This algorithm integrates Eq. 1 using the prescription

$$\begin{aligned} x(t+h) &= x(t) + c_1 h v(t) + c_2 h^2 F(x(t)) + \eta_1 \\ v(t+h) &= c_0 v(t) + c_1 h F(x(t)) + \eta_2 \end{aligned} \quad (4)$$

where

$$c_0 = e^{-\gamma h} \quad c_1 = \frac{1-c_0}{\gamma h} \quad c_2 = \frac{1-c_1}{\gamma h}$$

and where η_1 and η_2 are two random Gaussian variables with zero average and moments

$$\langle \eta_1^2 \rangle = \frac{T h}{\gamma} \left(2 - \frac{3 - 4e^{-\gamma h} + e^{-2\gamma h}}{\gamma h} \right)$$

$$\langle \eta_2^2 \rangle = T (1 - e^{-2\gamma h})$$

$$\langle \eta_1 \eta_2 \rangle = \frac{T}{\gamma} (1 - e^{-\gamma h})^2$$

The algebra to derive the correction to the equilibrium distribution induced by the numerical scheme in the general case and for a given high order integration scheme can be formidable; however, for a flow like Eq. 1 and for the scheme given by Eq. 4, the algebra is manageable. Assuming that (see Eq. 2, with $S \equiv S_1$)

$$P(x, v) = N \exp \left\{ - \left[v^2/2 + V(x) + hS(x, v) \right] / T \right\},$$

plugging the scheme of Eq. 4 into Eq. 3, we have that $S(x, v)$ satisfies the partial differential equation

$$\frac{\partial^2 S(x, v)}{\partial v^2} - \frac{v}{T\gamma} \frac{\partial S(x, v)}{\partial x} - \left(\frac{F(x)}{T\gamma} - \frac{v}{T} \right) \frac{\partial S(x, v)}{\partial v}$$

$$- \frac{v^2}{2\gamma T} F'(x) - \frac{1}{2\gamma} F'(x) = 0$$

This implies that this algorithm fails to reproduce the correct equilibrium distribution at $O(h)$ in the exponent. It is possible, for the case when $V(x) = \omega^2 x^2/2$, to solve this partial differential equation, obtaining the numerical equilibrium distribution at lowest order in h , which reads

$$P(x, v) = N \exp \left\{ - \left[v^2/2 + \omega^2 x^2/2 \right] / \hat{T} \right\}$$

with

$$\hat{T} = \frac{T}{1 + \frac{\omega^2 h}{2\gamma}}$$

i.e. the numerical equilibrium distribution is similar to the correct one, but with a renormalization of the temperature. In particular, this effective temperature (the temperature “simulated” by the algorithm) goes to zero in the limit $\gamma \rightarrow 0$. In [6] it is acknowledged that the algorithm does not work well in this limit, although no formal proof is provided.

To overcome the problem with the case of small γ , in [6] a second algorithm is proposed, which reads

$$\begin{aligned} x(t+h) &= x(t) + c_1 h v(t) + c_2 h^2 F(x(t)) + \eta_1 \\ v(t+h) &= c_0 v(t) + (c_1 - c_2) h F(x(t)) + \\ &\quad c_2 h F(x(t+h)) + \eta_2. \end{aligned} \quad (5)$$

Using Eq. 3 to evaluate the correction to the true equilibrium distribution generated by this algorithm, we find that the contribution S_1 vanishes, and we are left with the term S_2 . In other words, this algorithm reproduces the correct equilibrium distribution at $O(h)$, but there are still corrections $O(h^2)$ in the exponent. The algorithm given in Eq. 5 is the reference algorithm which we propose to improve in the next section. We will refer to this algorithm as “Li” (from *Liquid*) in the following.

III. QUASI SYMPLECTIC ALGORITHMS

A symplectic algorithm is a numerical scheme which attempts to preserve the 2-forms $dq_i \times dp_i$ during the integration of a Hamiltonian flow. The quantity q_i is a generalized coordinate, and p_i is the corresponding conjugate momentum. A nice introduction to the symplectic integration can be found in [14, 15]. Given the Hamiltonian $H(q_i, p_i)$, and the equations of motion

$$\dot{q}_i = \{q_i, H\} \quad \dot{p}_i = \{p_i, H\},$$

a symplectic integrator will in practice conserve some quantity \hat{H} , which in general reads

$$\hat{H} = H + h^n G(p_i, q_i)$$

where h is the integration time step, and G is a function which depends on the numerical scheme used for the integration. The problem of Hamiltonian flows in the presence of fluctuations has been addressed also in [11, 12],

whereas quasi symplectic schemes were derived in [13] (see also below, when various comparisons are carried out). A preliminary account of the material of this section can be found in [16].

Given that we are interested here in the integration of Eq. 1, we start from the symplectic integration of Hamiltonians which are separable and quadratic in the velocities. There are very many different possible symplectic schemes: however, having in mind that we are seeking a scheme which should be used in the integration of a stochastic differential equation, we restrict ourselves to considering a scheme in the form

$$q(i) = q(i-1) + ha_i p(i-1)$$

$$p(i) = p(i-1) + hb_i F(q(i))$$

for i between 1 and N , where $q(0) = q(t=0)$, $q(N) = q(t=h)$, etc., and h is the integration time step in the simulations. The coefficients $a(i)$ and $b(i)$ are chosen as to minimize, in some sense, the quantity $G(p, q)$.

The lowest possible symplectic algorithm one can write to integrate Eq. 1 following this approach reads when $\gamma = T = 0$ (this scheme is also known as “leap frog”)

$$\begin{aligned}\tilde{x} &= x(t) + \frac{h}{2}v(t) \\ v(t+h) &= v(t) + hF(\tilde{x}) \\ x(t+h) &= \tilde{x} + \frac{h}{2}v(t+h)\end{aligned}\quad (6)$$

where x is the position and v is the velocity. This scheme conserves the quantity $H - h^3(vFF' + v^3F''/6)/4$, where $H \equiv v^2/2 + V(x)$. It is then possible to reintroduce both the dissipation ($-\gamma v$) and the noise, writing the tentative scheme

$$\begin{aligned}\tilde{x} &= x(t) + \frac{h}{2}v(t) \\ v(t+h) &= c_2 [c_1 v(t) + hF(\tilde{x}) + d_1 \eta] \\ x(t+h) &= \tilde{x} + \frac{h}{2}v(t+h)\end{aligned}\quad (7)$$

where η is a Gaussian variable, with standard deviation one and average zero. We use again Eq. 3, and, imposing that the term $O(h)$ in the exponent (i.e. the term hS_1) vanishes, we find that the unknown arbitrary quantities c_1 , c_2 and d_1 read

$$\begin{aligned}c_1 &= 1 - \frac{\gamma h}{2} \\ c_2 &= \frac{1}{1 + \gamma h/2} \\ d_1 &= \sqrt{2T\gamma h}.\end{aligned}\quad (8)$$

Although we will carry out more extensive comparisons further down, let us briefly compare this scheme to the scheme of Eq. 5. The present scheme is by construction

well behaved in the limit of $\gamma \rightarrow 0$; it has the same accuracy in computing the equilibrium distribution as of Eq. 5; but it requires only one random deviate per integration time step (as opposed to two deviates for the scheme of Eq. 5), so it will run faster. In the following, we will refer to the algorithm of Eq. 7 as “SLO” (Symplectic Low Order).

Looking at the structure of the previous algorithm, we can try to derive an algorithm of higher order. In the derivation of Eq. 7, when we applied Eq. 3, given the number of unknown quantities we could only impose that the term $O(h)$ in the exponent disappeared. If we could somehow increase the number of unknown quantities when applying Eq. 3, while keeping the algorithm simple, we might be able to make the terms $O(h^2)$ in the exponent disappear. We start combining two steps, each one of the form of Eq. 7, done with an integration time step $h/2$,

$$\begin{aligned}x_1 &= x(t) + \frac{h}{4}v(t) \\ v_1 &= c_2 \left[c_1 v(t) + \frac{h}{2}F(x_1) + \sqrt{\gamma Th}(a_1 \eta_1 + a_2 \eta_2) \right] \\ x_2 &= x_1 + \frac{h}{2}v_1 \\ v(t+h) &= c_2 \left[c_1 v_1 + \frac{h}{2}F(x_2) + \sqrt{\gamma Th}(b_1 \eta_1 + b_2 \eta_2) \right] \\ x(t+h) &= x_2 + \frac{h}{4}v(t+h)\end{aligned}\quad (9)$$

where $c_1 = (1 - \gamma h/4)$ and $c_2 = 1/(1 + \gamma h/4)$. Here, η_1 and η_2 are two random Gaussian variables of standard deviation one and average zero. The idea is now to choose the coefficients a 's and b 's in such a way as to annihilate S_1 , and possibly minimize S_2 . This is done using Eq. 9 in Eq. 3, which results in a number of algebraic equations for a_i and b_i . The algebra, although straightforward, is cumbersome and we will simply report here the results. For a given a_1 , the following choice for the other three parameters will ensure that S_1 vanishes identically:

$$\begin{aligned}b_1 &= -\frac{a_1}{7} + \frac{2\sqrt{14 - 12a_1^2}}{7} \\ b_2 &= -\frac{\sqrt{7 + 282a_1^2 + 24a_1\sqrt{14 - 16a_1^2}}}{\sqrt{42}} \\ a_2 &= \frac{\sqrt{42}b_2(-7\sqrt{2} + 6\sqrt{2}a_1^2 + 24a_1\sqrt{7 - 6a_1^2})}{\sqrt{3}(-14 + 588a_1^2)}.\end{aligned}$$

As function of a_2 , we can now write the equations satisfied by S_2 : we find that S_2 vanishes for a particular choice of the parameter a_2 . Summarizing the numerics, the set of a 's and b 's which simultaneously makes S_1 and S_2 vanish are:

$$a_1 = -1.0691860043307065\dots$$

$$\begin{aligned}
a_2 &= -0.1533230407019893\dots \\
b_1 &= 0.3044913128854065\dots \\
b_2 &= -1.0363164126095790\dots
\end{aligned} \tag{10}$$

The conclusion is that the algorithm given by Eqs. 9 and 10 is symplectic in the limit $\gamma \rightarrow 0$ (conserving the quantity $H - h^3(vFF' + v^3F''/6)/16$), whereas for a finite γ it reproduces the correct equilibrium distribution with an error $O(h^3)$ in the exponent. We will refer to this algorithm as to “SHO” (Symplectic High Order).

In the following, we will use also the Heun algorithm to carry out the various comparisons. To make this paper as self contained as possible, we recall here that the Heun algorithm for a system like the one in Eq. 1 is given by the prescription:

$$\begin{aligned}
x_1 &= x(t) + hv(t) \\
v_1 &= v(t) - h\gamma v(t) + hF(x(t)) + \sqrt{2\gamma Th\eta} \\
x_2 &= x(t) + hv_1 \\
v_2 &= v(t) - h\gamma v_1 + hF(x_1) + \sqrt{2\gamma Th\eta} \\
x(t+h) &= \frac{x_1 + x_2}{2} \quad v(t+h) = \frac{v_1 + v_2}{2}
\end{aligned}$$

The Heun algorithm does not make use of the (quasi) symplectic nature of the flow: we expect that it will not fare too well in the limit of small γ . We recall that it is known [5] that the equilibrium distribution generated by the Heun algorithm is accurate up to $o(h^2)$ in the exponent. We will refer to the Heun scheme as to “He”.

We will also compare our algorithms to the quasi symplectic algorithms of [13]: we should mention here that really the latter are weak integration schemes (for a definition of weak and strong integration schemes, see [2]), hence they are bound to give worse results than the other schemes when, as we do, average quantities are considered. The two algorithms considered integrate with the prescriptions ([13] should be consulted for more details):

MT1:

$$\begin{aligned}
x(t+h) &= x(t) + hv(t+h) \\
v(t+h) &= v(t) - hV'(x(t+h)) - h\gamma v(t+h) \\
&\quad + \sqrt{2Th\gamma\eta}
\end{aligned} \tag{11}$$

where $v(t+h)$ and $x(t+h)$ should be found recursively.

MT2:

$$\begin{aligned}
v(t+h) &= (1 - \gamma h)(v(t) - hV'(x(t)) + \sqrt{2Th\gamma\eta}) \\
x(t+h) &= x(t) + h(v(t) - hV'(x(t)))
\end{aligned} \tag{12}$$

The random variables η take the values ± 1 . These variables are faster to generate than a Gaussian variable, hence these algorithms will run faster, allowing for a smaller integration timestep to compensate for less accuracy when averaged quantities are considered. However,

having said this, if we used Eq. 3 to assess these two algorithms, we would find that they both have a correction to the equilibrium distribution $O(h)$ in the exponent: these will reflect in the numerical experiments, as we will comment below.

Finally, it should be noted that given the structure of the Hamiltonian in the limit $T \rightarrow 0$ and $\gamma \rightarrow 0$, which is $H = v^2/2 + V(x)$, the equilibrium distribution for Eq. 1 can also be written as

$$P(x, v) \propto \exp -H/T.$$

At first sight, it may appear that the request of a symplectic integration scheme is redundant, once we made sure that the “correct” equilibrium distribution is generated in the numerical integration. This is not right: the limit $T \rightarrow 0$ is singular, hence a symplectic form for the numerical scheme can (and should) be imposed as an additional condition.

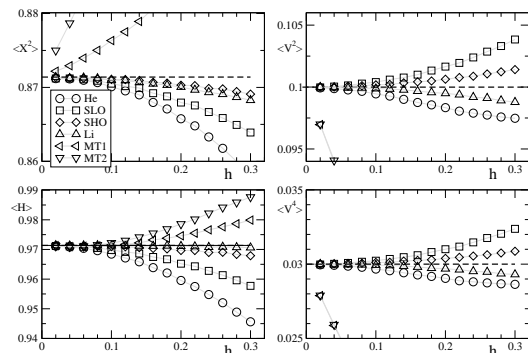


FIG. 1: Result of simulations for different integration schemes, as function of the integration time step h , for the system in Eq. 14. Various moments are considered (see text for details), taking $T = 0.1$ and $\gamma = 1$

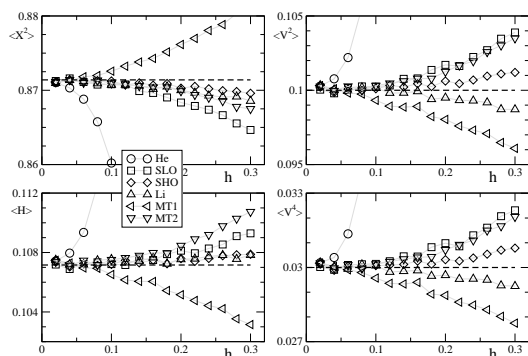


FIG. 2: Result of simulations for different integration schemes, as function of the integration time step h , for the system in Eq. 14. Various moments are considered (see text for details), taking $T = 0.1$ and $\gamma = 10^{-2}$

IV. NUMERICAL EXPERIMENTS

We compare now the results of applying the algorithms described previously to the integration of two prototype stochastic differential equations. Let us first consider how the different algorithms reproduce the equilibrium properties: to this end, we integrate the equations of motion, and compute some equilibrium momenta, which are then compared to the theoretical ones.

The first system studied is given by

$$\begin{aligned} \dot{x} &= v \\ \dot{v} &= -\gamma v - V'(x) + \sqrt{2\gamma T}\eta \\ V(x) &= x^4/4 - x^2/2 \end{aligned} \quad (13)$$

For this system we fixed the noise intensity to $T = 0.1$, and carried out the numerical integration for two different values of the damping coefficient γ and for the different integration schemes. The results are summarized in Fig. 1 (for $\gamma = 1$) and in Fig. 2 (for $\gamma = 10^{-2}$). The quantity $\langle H \rangle$ is defined as $\langle H \rangle \equiv \langle v^2/2 + V(x) \rangle$. In all figures, the results of the digital simulations are shown by symbols with a gray straight line as guide to the eye; the bold dashed line is the expected (theoretical) value for the quantity considered. For the number of averages considered, the statistical error is much smaller than (order of) the symbols for the larger (smaller) damping.

Let us comment the results. It is evident that the Heun method (He in figures) is not very appropriate for the smaller damping considered (Fig. 2). Even for the larger damping (Fig. 1), the Heun algorithm is typically outperformed by the Symplectic Low Order scheme (SLO, Eq. 7); note that the SLO is fairly faster than He, given that it requires only one evaluation of the deterministic force for each integration time step.

The algorithms MT1 and MT2, as expected, do not work well for the larger damping considered, and become more accurate as the damping is reduced: it should be noted that for this case, MT2 seems to be more accurate than MT1 for a given integration time step: considering that MT2 is much faster than MT1, the conclusion seems to be that MT2 ought to be preferred, between these two schemes. Note also that the error on the moments for these two schemes seems to grow linearly with the integration time step h , which is related to the $O(h)$ error in the exponent which was mentioned in the previous section.

The Li algorithm is less accurate than SHO when the x^2 moments are considered: for both values of the damping in the whole h region. The Symplectic High Order (SHO) is the algorithm which gives the most accurate results for the x^2 moment, and results comparable or better than to the one obtained with Li for the v^2 and v^4 moments. It is only when $\langle H \rangle$ is considered, and for the larger damping, that Li seems to be more accurate than SHO. However, care is necessary in drawing conclusions from $\langle H \rangle$: looking for instance at Fig. 1, we note that Li underestimates both v^2 and x^2 : recalling the struc-

ture of the potential $V(x) = -x^2/2 + x^4/4$, it is clear that these two underestimates tend to cancel out, leading to a $\langle H \rangle$ closer to the theoretical one, but only by virtue of a coincidental cancellation.

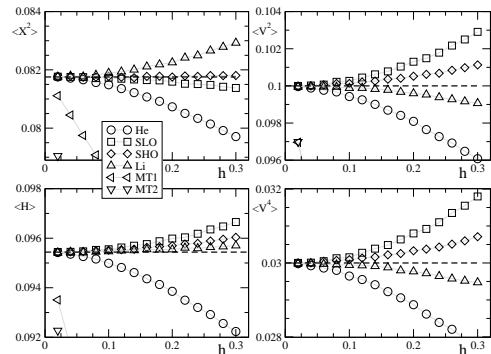


FIG. 3: Result of simulations for different integration schemes, as function of the integration time step h , for the system in Eq. 15. Various moments are considered (see text for details), taking $T = 0.1$ and $\gamma = 1$

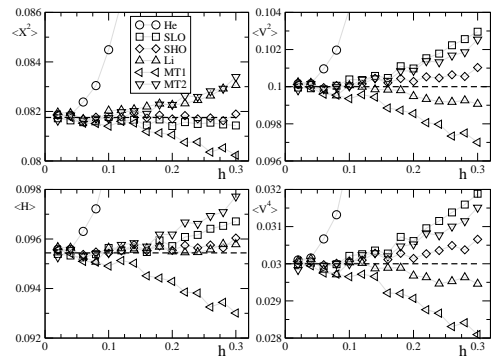


FIG. 4: Result of simulations for different integration schemes, as function of the integration time step h , for the system in Eq. 15. Various moments are considered (see text for details), taking $T = 0.1$ and $\gamma = 10^{-2}$

The second system studied is similar to the first one:

$$\begin{aligned} \dot{x} &= v \\ \dot{v} &= -\gamma v - V'(x) + \sqrt{2\gamma T}\eta \\ V(x) &= x^4/4 + x^2/2 \end{aligned} \quad (14)$$

the only difference with the system of Eq. 14 being that now the potential is monostable.

The result of the computer experiments are summarized in Figs. 3 and 4. The comments parallel the comments we already made for the system of Eq. 14. Heun (He) is the least accurate scheme for small damping, although the error on the moments is quadratic on h (a

signature of an $O(h^2)$ error in the equilibrium distribution). MT1 and MT2 perform better at smaller damping, with an error on the moments which is roughly linear in the integration time step. SLO does better than both He and MT1, MT2, and for both damping considered, being as fast (if not faster) than both schemes. When the x^2 is considered, Li appears to perform worse than even SLO. SHO outperforms Li: only when H is considered, Li seems to be more accurate than SHO, but again only by virtue of a cancellation (again, between $\langle x^2 \rangle$ and $\langle v^2 \rangle$).

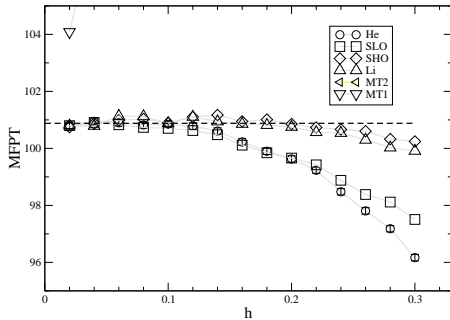


FIG. 5: Result of simulations for different integration schemes, as function of the integration time step h , for the system in Eq. 14. The Mean First Passage Time between the minima is considered (see text for details), taking $T = 0.1$ and $\gamma = 1$

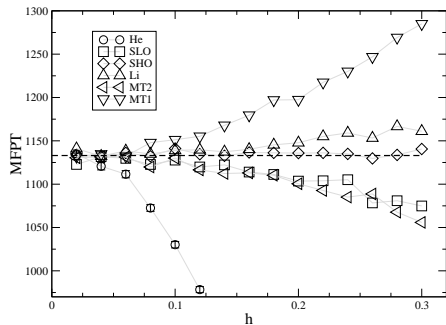


FIG. 6: Result of simulations for different integration schemes, as function of the integration time step h , for the system in Eq. 14. The Mean First Passage Time between the minima is considered (see text for details), taking $T = 0.1$ and $\gamma = 10^{-2}$

We turn now to some numerical experiments to assess how the various algorithms perform when dynamical quantities are considered. Using the system of Eq. 14, we computed the Mean First Passage Times (MFPT) to go from one of the minima to the other one (the minima

are located at $x = \pm 1$): the results of the simulations are summarized in Figs. 5 and 6. Given the fairly large value of the noise intensity ($T = 0.1$), there is no theory available to compute an “exact” MFPT for comparison with the simulated MFPTs. To have some reference, we took as reference value the average of the MFPT obtained via the algorithms Li and SHO for the three smallest h values used in the simulations, and drew the dashed line at this value. The expected statistical error, due to the finiteness of the sample used, is of the order of the symbol size. For the larger damping considered (Fig. 5, $\gamma = 1$), He and SLO perform in a similar way. MT1 and MT2 give unreasonable values for the MFPT (only one point for MT1 is actually on the graph, for the smallest h considered: all other points for both algorithms are outside the MFPT range considered). Li and SHO perform in a similar way, giving results closer to the “correct” MFPT throughout the h range considered, with a slightly better agreement shown by SHO for larger h 's. The situation is more interesting when a smaller damping is considered (Fig. 6, $\gamma = 10^{-2}$). While showing an error which grows only quadratically in h , clearly He is the algorithm which performs worse. MT1 and MT2 now give more reasonable results, and they yield MFPT comparable to the ones obtained using SLO. SHO outperforms Li, giving MFPT closer to the “exact” ones over the whole h range considered. Li on the other hand seems to give results which are roughly equivalent to the ones obtained using MT1, MT2 or SLO.

We would like to conclude noting that the numerical experiments were done stretching the algorithms into parameter regions which are somehow extreme: the typical time scale for the potential considered is around 0.5 (the oscillation frequency around the minima for Eq. 14) or around 1 (the larger γ considered, and the oscillation frequency for the potential of Eq. 15), and yet an algorithm like SHO is able to integrate up to integration time steps h order of 0.3, with corrections to the moments or to the MFPTs which are smaller than, or at worse order of 1%: in our opinion, these are remarkable results, particularly when the flatness of the MFPT computed with SHO in Fig. 6 is considered.

V. CONCLUSIONS

We introduced two algorithms for the numerical integration of the equations of motion of a Brownian walker. The features of these algorithms are that they become symplectic when the damping on the Brownian walker is taken to be zero, and give the correct equilibrium distribution to some higher order in the integration time steps for a finite damping and temperature. This, in turn, leads to more accuracy when dynamical quantities are considered (like the MFPT). Possible applications of these algorithms, beside the mentioned generic integration of the dynamics in the liquid state [6], are in the integration of the dynamical equations of ions moving in

and around ionic channels [18]: here the speed up provided by algorithms which are stable for fairly large time

steps may help in improving current simulations.

-
- [1] For a classical introduction, see *Noise in nonlinear Dynamical Systems*, vols 1, 2 and 3, F. Moss and P. V. E. McClintock eds., Cambridge University Press, 1989.
- [2] P. E. Kloeden and E. Platen, *Numerical simulation of stochastic differential equations* Springer-Verlag Berlin, 1992
- [3] J. Garcia-Ojalvo and J. Sancho, *Noise in Spatially Extended Systems* Springer-Verlag Berlin, 1999
- [4] G. N. Milstein and M. V. Tretyakov *SIAM J. Num. Anal.* **34** 2142–2176 (1997)
- [5] R. Mannella, *Int J Mod Phys C* **13** 1177–1194 (2002)
- [6] M. P. Allen and D. J. Tildesley, *Computer Simulation of Liquids* Oxford University Press, 2001
- [7] A. C. Brañka and D. M. Heyes, *Phys Rev E* **60** 2381–2388 (1999)
- [8] H. A. Forbert and S. A. Chin, *Phys Rev E* **63** 016703 (2000)
- [9] Ji Qiang and S. Habib, *Phys Rev E* **62** 7430–7437 (2000)
- [10] W. Paul and D. Y. Yoon, *Phys Rev E* **52** 2076–2083 (1995)
- [11] G. N. Milnstein and M. V. Tretyakov, “Numerical methods for Langevin type equations based on symplectic integrators”, *Preprint 727*, Weierstrab-Institut für Angewandte Analysis und Stochastik, Berlin (2002).
- [12] G. N. Milnstein, Yu. M. Repin and M. V. Tretyakov, *SIAM J Numer Anal*, **40** 1583-1604 (2003).
- [13] G. N. Milnstein and M. V. Tretyakov, *IMA J Numer Anal*, **23** 1-34 (2003).
- [14] H. Yoshida, *Phys Lett A* **150** 262–268 (1990)
- [15] J. M. Sanz-Serna, *Acta Numerica* **1** 243–286 (1991)
- [16] R. Mannella, in *Supercomputation in nonlinear and disordered systems*, L. Vasquez, F. Tirado and I. Martin eds (World Scientific) 100–129 (1997).
- [17] G. G. Batrouni, G. R. Katz, A. S. Kronfeld, G. P. Lepage, B. Svetitsky and K. G. Wilson, *Phys Rev D* **32** 2736 (1985)
- [18] G. Moy, B. Corry, S. Kuyucak and S.-O. Chung, *Biophys J* **78**, 2349–2363 (2000); B. Corry, M. Hoyles, T. W. Allen, M. Walker, S. Kuyucak and S.-H. Chung, *Biophys J* **82** 1975–1984 (2002).